Natural Resources for Human Health
eISSN: 2583-1194

Original Research

**Received** 22 April 2026
**Revised** 20 May 2026
**Accepted** 14 June 2026

Natural Resources for Human Health 2026, Vol. 6 (3s): 866–875

**KEYWORDS**:
Forest Fire Smoke Detection; Deep Learning; Air Pollution Mapping; Satellite Remote Sensing; U-Net Segmentation; Health-Risk Assessment

# An Advanced Deep Learning Framework for Mapping Forest Fire Smoke and Air Pollution Impacts on Human Health Using Satellite Imagery

Dr. Ninad Narayan More[1], Dr. Divya Chakkaravarthy[2], Dr. Swapnali Makdey[3], Dr Ankush Balaram Pawar[4], Dr. Avinash Raut[5]

[1]Post-Doctoral Research Scholar, Department of Computer Science and Engineering, Lincoln University College, Kelana Jaya, 47301, Malaysia.
ninadmore.pdf@lincoln.edu.my
[2]Principal Supervisor, School of AI Computing and Multimedia, Lincoln University College, Kelana Jaya, 47301, Malaysia.
divya@lincoln.edu.my
[3]Associate professor, Department of Electronics and Computer science,
Fr. Conceicao Rodrigues college of Engineering, Mumbai, Maharashtra-400050, India.
swapnali@frcrce.ac.in
[4]Associate Professor, Computer Engineering Department, Anjuman I Islam's Kalsekar Technical Campus, School of Engineering & Technology, New Panvel, Maharashtra 410206, India.
ankush.pawar@aiktc.ac.in
[5]Department of Engineering, Science and Humanities, Vishwakarma Institute of Technology, Pune, Maharashtra, India.
avinash.raut@vit.edu

**ABSTRACT:** The smoke produced during forest fires is a large-scale plume that contains high levels of hazardous air pollutants (HAPs) that can affect a wide geographical area and cause environmental and public-health problems. Traditional monitoring systems, however, only monitor at a small number of spatial locations, and they are not always sufficient for determining population level smoke exposure. In this study, an advanced deep learning approach is suggested to extract information about forest-fire smoke, air pollution, and impacts on human health from multispectral satellite data and observations from the atmosphere. This framework combines the spatial feature extraction by Convolutional Neural Networks (CNNs) with the segmentation of smoke-plumes by U-Net and the spatiotemporal analysis of pollution by Long Short-Term Memory (LSTM) networks. Satellite-based aerosol optical depth, fire radiative power, land surface temperature, vegetation indices, PM2.5 and air quality observations are combined to define exposure intensity. The experimental results show that the mapping of smoke affected areas is accurate with 96.75%, precise with 96.18%, recalled with 95.62%, F1 score with 95.90% and AUC with 0.982, and IoU with 93.84%. The novelty of the approach is related to the integration of fire detection, segmentation, estimation of pollution and mapping of health risk in a given architecture. The framework delivers scalable identification of pollution hotspots and communities with high exposures. The results show its potential in the support of early health advice, environmental surveillance, data-driven disaster-response planning.

## I. INTRODUCTION

Global climate changes, extended dry seasons and higher fuel load in forest landscapes have led to an increase in forest fires in terms of both their occurrence, severity and duration [1]. In addition to immediate ecological damage, fires emit tremendous amounts of smoke consisting of particulates, carbon monoxide and VOCs which can be many hundreds of kilometers from the burn area and therefore have impacts well outside the perimeters of the fire itself [2]. Exposure to these smoke plumes increases the risks for respiratory disease, cardiovascular stress, and premature death, especially for children, elderly people and people with underlying health conditions [3]. Ground-based air-quality monitoring networks are accurate and provide high frequency measurements at fixed locations, but are sparse, and do not sample the spatial distribution of smoke dispersion and can not provide information about exposures to many high-risk communities in a timely manner [4]. Satellite remote sensing, on the other hand, provides continuous wide area coverage, which is suitable for identifying active fires, monitoring the development of the smoke plumes, and estimating aerosol loading in near real-time, and is readily scalable [5]. The recent progress in deep learning has also led to the ability of automatically extracting complex spatial and temporal pattern from the multispectral imagery, which is more capable than using traditional pixel-based or threshold classification methods [6]. Most of the current systems however rely on tackling the problems of fire detection, smoke segmentation and pollution estimation separately and not have a common pipeline that takes environmental observations to public health results [7].

### A. Research Problem and Objectives

This gap inspired the present study, aiming to develop an integrated deep-learning framework for simultaneous detection of forest-fire smoke, segmentation of affected areas, estimation of pollutant concentration and mapping of the resulting health risk directly from data acquired from satellites.

### B. Novelty and Contributions

The proposed approach is novel since it integrates CNN-based spatial feature extraction, U-Net segmentation, and LSTM-based temporal pollution modeling in one end-to-end architecture to predict end-to-end maps of actionable health risks instead of individual scores of detection.

**Key Contributions:**

- Proposes a unified CNN–U-Net–LSTM framework that simultaneously detects the smoke, segments the smoke plume and forecasts pollution from Sentinel-2 satellite images.
- Adds a health-risk mapping module that transforms the spatiotemporal estimates of pollution levels into classes of pollution exposure for vulnerable population living in the proximity of fire zones.
- By a detailed experimental comparison, showcases the ability to deliver excellent accuracy, segmentation overlap and pollutant-estimation results when compared with the conventional machine-learning and single-model deep-learning baselines.

## II. RELATED WORK

Until recently, the early detection of fire in the satellite era was based on thermal-anomaly thresholds of MODIS and VIIRS data, which provided global coverage but were not adequate for small or smouldering fires [8]. This approach has since been extended to Sentinel-2 and Landsat images, with the aim of enhancing the delineation of the fire-front and the detection of the boundaries of the smoke-plumes for varying illumination and cloud conditions [9]. The combination of optical and thermal channels (multi-sensor fusion) further improved the robustness of detection, across various biomes and seasons [10]. A thorough survey of these techniques points out that there is an ongoing problem with producing a distinction between thin smoke and haze and also between haze and cloud cover, which encourages architectures which are explicitly formulated for the segmentation of smoke plumes and do not have to distinguish between smoke and cloud cover [11].

The deep networks have been applied to mapping air pollution as well by correlating the aerosol optical depth and meteorological parameters with the air pollution concentration at ground level, which often gave better performance than other regression-based chemical transport models [12]. Spatial and spectral fusion architectures using several sensors have shown to have better estimation accuracy for particulate and gaseous pollutants during a wildfire event [13]. Pollutant concentration time series data after fire has been dispersed shows temporal evolution following the onset of the fire, and is well suited to recurrent architectures such as LSTM networks because the dispersion and settling of the smoke are sequential phenomena.

For health impact, a number of studies have associated satellite-derived pollution indices with hospitalisation records for respiratory and cardiovascular diseases, thus providing quantitative exposure-response relationships for wildfire smoke for these specific diseases [15]. There have also been machine-learning based air-quality-index prediction systems that have been employed to produce a localised advisory, although most of them are not fire or smoke source attribution based.

## III. DATASET AND DATA PREPROCESSING

### A. Satellite Imagery and Environmental Data

In this study, the Copernicus Sentinel-2 Multispectral Instrument (MSI) is the main imaging instrument used, providing several spectral bands in the visible, near-infrared and short-wave infrared with spatial resolutions of 10 m, 20 m and 60 m, and a five day revisit frequency. Six bands covering the areas of relevance to fire and vegetation characterization were extracted for each scene: the Band 2 (Blue), Band 3 (Green), Band 4 (Red), Band 8 (Near-Infrared), and two Shortwave-Infrared bands (B11, B12), which are sensitive to the surface reflectance and the spectral signatures of active fire and smoke aerosols, respectively. Surface-reflectance products, corrected to remove the effects of the atmosphere, were used at level-2A to minimize the atmosphere before tiling.

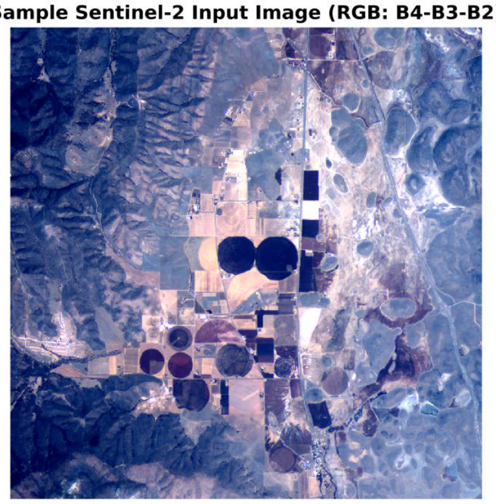


**Figure 1.** Sample Sentinel-2 True-Color Input Image (Bands 4-3-2) Used as Model Input

The true-color Sentinel-2 composite presented in figure 1 is a representative example of the data used as input for the model, and represents the forested area with localized variation in reflectance that is found in the study area, before band-wise pre-processing and tiling steps.

### B. Air Quality and Health-Related Data

The pollution-estimation module was supervised using ground-station observations of PM2.5, PM10 and Air Quality Index (AQI) from area-wide environmental monitoring networks that were temporally correlated with the satellite overpass data. Aerosol Optical Depth (AOD) retrievals were used as a surrogate between the satellite reflectance and the concentration of pollutants at the Earth's surface. The exposure-severity classes used for training the health-risk mapping component were created using health-related indicators, such as population-density layers, and public health and census data, including respiratory-illness hospital admission rates.

### C. Data Preprocessing and Feature Extraction

All satellite bands were co-registered, resampled to a common 10 m resolution, and cropped into 256×256 pixel tiles, to make the dimensions of the inputs to the CNN, U-Net and LSTM sub-networks uniform. To scale reflectance values to a common range, reducing the effect of variations in sensor and illumination, a radiometric normalization was applied, as in Equation (1).

To improve discrimination between burned area, healthy canopy and smoke-obscured pixels, vegetation and burn sensitive indices such as the Normalized Difference Vegetation Index (NDVI) were calculated as in Equation (2): The cloud and bad pixels were masked by applying Sentinel-2 scene classification layer and temporal sequences of five consecutive acquisitions were stacked to give spatiotemporal context to the LSTM module to estimate the trend of pollutant.

$$I_{norm} = \frac{I - I_{min}}{I_{max} - I_{min} + \varepsilon} \tag{1}$$

$$NDVI = \frac{\rho_{NIR} - \rho_{Red}}{\rho_{NIR} + \rho_{Red}} \tag{2}$$

## IV. METHODOLOGY

The proposed solution consists of three deep-learning modules: a CNN to extract spatial features, a U-Net to segment the smoke-plumes at a pixel level and a LSTM network for the spatiotemporal simulation of pollution. The features extracted and pollutant estimates are then combined in a health risk mapping module which categorizes the level of exposure in the observed area.

### A. Proposed Deep Learning Framework Architecture

This proposed framework is a sequential, but connected, pipeline that would bring multispectral satellite observations to the stage of providing information on health risk. The pre-processed Sentinel-2 tiles are then input to a convolutional neural network (CNN) backbone that captures the hierarchy of the spatial features associated with the edges, textures, and spectral gradients of the active fire fronts, burned vegetation and smoke aerosols. They include maps that are passed to a U-Net encoder-decoder network that uses skip connections for retaining fine spatial detail, and outputs a binary plume mask at the resolution of the original image, which is segmented on a per-pixel basis for smoke-affected areas. The sequential picture flow of information from the Sentinel-2 data to the feature extraction block (CNN), to the next segmentation block (U-Net), and the next temporal pollution modelling block (LSTM), with the final output being the health-risk mapping, is shown in Figure 2, distinguishing this picture flow from previous isolated-task approaches.

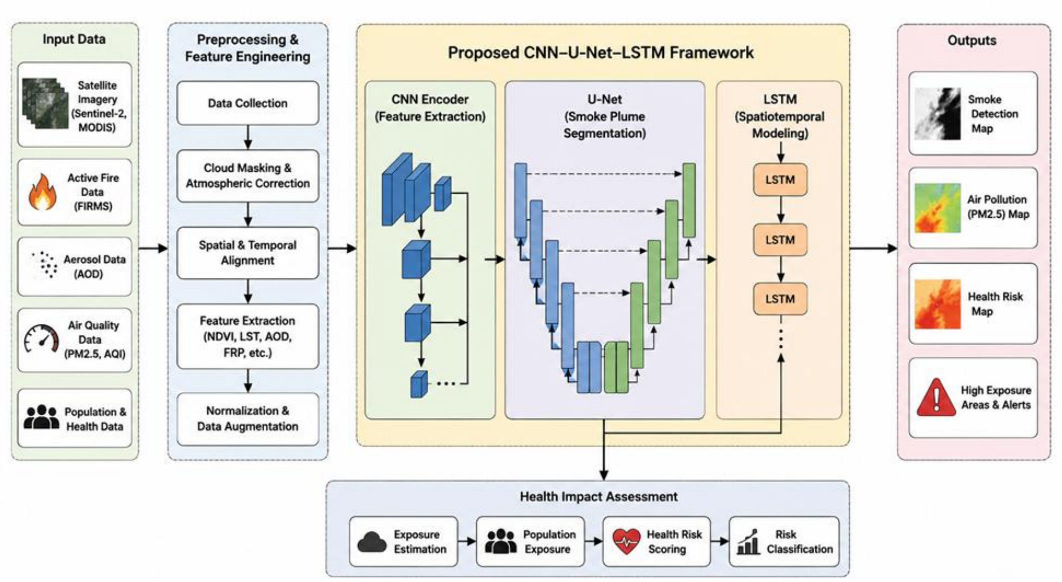


**Figure 2.** Block Diagram of the Proposed Deep Learning Framework

### B. CNN-Based Spatial Feature Extraction

The CNN backbone consists of 4 convolutional blocks, which have 32, 64, 128 and 256 filters, respectively, followed by ReLU activation and batch normalization for block-wise normalization, and max-pooling for progressive downsampling in space. This hierarchy is able to detect low-level (edge and texture) information in early layers and high-level (fire and smoke related) spectral patterns in deeper layers, which result in feature maps that are then passed on to the segmentation and temporal modules.

$$F_k = \sigma(W_k * X_{k-1} + b_k) \tag{3}$$

**Algorithm 1: CNN-Based Spatial Feature Extraction**

Input: Preprocessed Sentinel-2 tile $X \in \mathbb{R}^{256x256x6}$

Output: Feature map F

1: $F_0 \leftarrow X$

2: for k = 1 to 4 do

3: $C_k \leftarrow$ Conv2D($F_{k-1}$, filters = {32,64,128,256}[k], kernel = 3×3)

4: $B_k \leftarrow$ BatchNorm($C_k$)

5: $A_k \leftarrow$ ReLU($B_k$)

6: $F_k \leftarrow$ MaxPool2D($A_k$, pool = 2×2)

7: end for

8: return $F_4$

**C. U-Net-Based Smoke Plume Segmentation**

The U-Net module takes CNN output feature maps and implements a symmetric encoder-decoder architecture having four downsampling and four upsampling layers. Skip connections link together the feature maps from the encoder to the layers in the decoder, maintaining more detail in the plume boundaries for regions that are not downsampled. The last convolution block has a sigmoid activation function which gives a smoke-mask output, and is trained with a combination of binary cross-entropy and Dice loss, which is a compromise between pixel-wise accuracy and region overlap.

$$L_{seg} = L_{BCE} + L_{Dice} = -\sum_i y_i \log(yp_i) + \left(1 - \frac{2\sum_i y_i yp_i}{\sum_i y_i + \sum_i yp_i}\right) \tag{4}$$

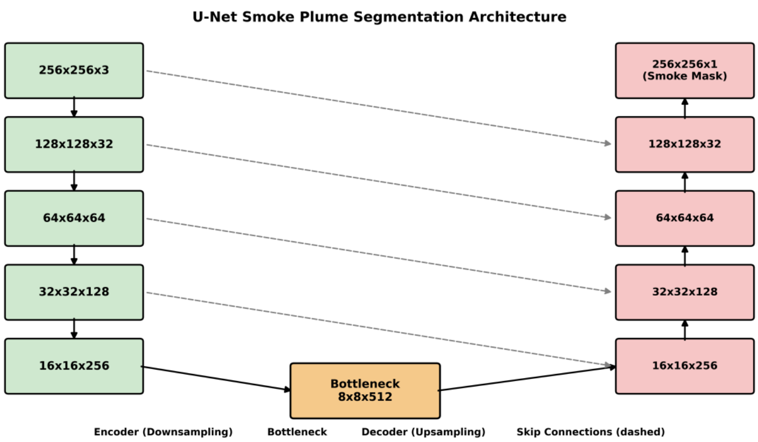


**Figure 3.** U-Net Architecture for Smoke Plume Segmentation

The U-Net architecture is shown in Figure 3, where the encoder gradually down-samples the spatial resolution and up-samples the feature depth; the bottleneck that gathers the information from the entire image; and the decoder that restores the image resolution by transposed convolution with the help of skip connections, which provide precise delineation of the smoke-plumes at their full image resolution.

**D. LSTM-Based Spatiotemporal Pollution Analysis**

The model takes 5 consecutive Sentinel-2 images as input, and is composed of 2 layers of LSTMs, each with 128 hidden units, which allows the model to capture the temporal relationships in the data for smoke dispersion and pollutant accumulation. The

LSTM cells control entry, forgetting and output of information, enabling the network to keep relevant information of the past and then forget or remove noise caused by a fleeting cloud cover or sensor quirks. The last hidden layer passes through fully connected layers for regression of the PM2.5, PM10, AOD and AQI values resulting in continuous spatially resolved pollution estimates, in addition to the static segmentation output.

$$h_t = o_t \odot \tanh(C_t) \tag{5}$$

## V. EXPERIMENTAL RESULTS AND ANALYSIS

A complete assessment of the proposed framework for all the tasks involved in the smoke detection, segmentation, estimation of pollution and classification of health-risk is presented in this section. The performance is compared to four base models (Random Forest, standalone CNN, ResNet50, U-Net and CNN-LSTM) with reference to standard classification and regression metrics. As illustrated in Tables 2-6 and the associated figures, the CNN-U-Net-LSTM model consistently outperforms the single-task counterparts, showing that multi-task learning is beneficial.

### A. Experimental Setup and Evaluation Metrics

The experiments were run with the hyperparameters listed below in Table 1, with an input tile size of 256×256, a batch size of 32, Adam optimizer with a learning rate of 0.0001 and a BCE-Dice loss that was trained for 100 epochs using a train/val/test split of 70:15:15. For classification based tasks, the accuracy, precision, recall, F1 score and area under the ROC curve (AUC) were used to evaluate the performance of the model, while the Intersection-over-Union (IoU) was used for assessing the performance of the segmentation tasks, both of which were formulated in Equations (6) through (9).

**Table 1.** Key Hyperparameters of the Proposed Framework

| Hyperparameter | Value |
|---|---|
| Input Image Size | 256 × 256 |
| CNN Filters | 32, 64, 128, 256 |
| U-Net Depth | 4 |
| LSTM Units | 128 |
| Dropout Rate | 0.30 |
| Batch Size | 32 |
| Learning Rate | 0.0001 |
| Optimizer | Adam |
| Loss Function | BCE + Dice Loss |
| Epochs | 100 |
| Data Split | 70:15:15 |

### B. Smoke Detection Performance

Table 2 shows the comparison of proposed CNN-U-Net-LSTM framework with 5 baseline methods of smoke detection. The proposed model not only achieves the highest accuracy of 96.75%, but also the best precision of 96.18%, recall of 95.62%, F1-score of 95.90% and AUC of 0.982 when compared to the next best CNN-LSTM baseline by an average of around 1.3 percentage points in accuracy. Random Forest shows the lowest results on all metrics, thus demonstrating its weak performance in capturing the complexity of the spectral and spatial characteristics of smoke signatures, which makes it difficult for classical models to achieve good performance in such cases. The margin just over the whole precision-recall curve suggests that the proposed architecture not only minimizes false positives, but also minimizes missed detections without sacrificing an improvement in precision.

Natural Resources for
Human Health
eISSN: 2583-1194

**Table 2.** Comparative Performance Analysis

| Method | Accuracy (%) | Precision (%) | Recall (%) | F1-Score (%) | AUC |
|---|---|---|---|---|---|
| Random Forest | 87.42 | 86.73 | 85.91 | 86.32 | 0.902 |
| CNN | 91.68 | 90.84 | 90.21 | 90.52 | 0.934 |
| ResNet50 | 93.27 | 92.65 | 91.94 | 92.29 | 0.951 |
| U-Net | 94.36 | 93.71 | 93.28 | 93.49 | 0.963 |
| CNN-LSTM | 95.42 | 94.86 | 94.31 | 94.58 | 0.974 |
| **Proposed CNN-U-Net-LSTM** | **96.75** | **96.18** | **95.62** | **95.90** | **0.982** |

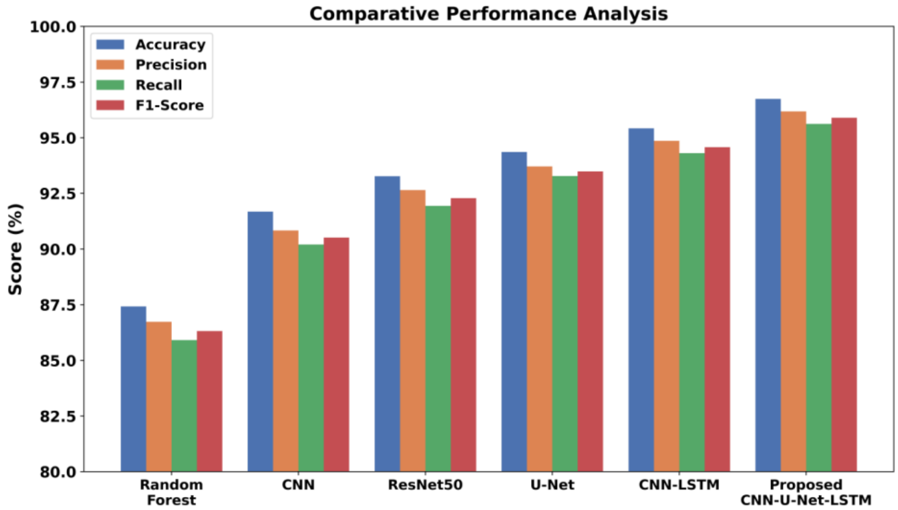


**Figure 4.** Comparative Performance Analysis across Methods

The comparative bar chart of accuracy, precision, recall and f1 score of all 6 methods is displayed in figure 4, where the accuracy of the proposed method is observed to be at the peak bar with every evaluation metric, showing that the accuracy is improving progressively from random forest to single model deep architectures to the proposed integrated method.

**C. Smoke-Affected Area Segmentation**

The pixel-level segmentation quality for mapping of smoke-affected areas is shown in Table 3. The proposed framework achieves an IoU of 93.84% and Dice score of 96.12% which is 2.57% and 1.94% higher than that of CNN-U-Net variant, respectively, and significantly better than the standalone U-Net. The CNN extracted feature maps are also passed into the U-Net decoder and the pixel accuracy of 97.16% and segmentation precision of 96.08% further indicate that boundary delineation can be improved with the CNN extracted feature maps. The improvements also show that, as the first time co-optimizing spatial features in the hierarchy and skip-connections in the decoding can generate sharper, more spatially coherent smoke masks than segmentation-only architectures, a key component for accurate estimation of the geographic area that is exposed.

**Table 3. Smoke-Plume Segmentation Performance**

| Parameter | U-Net | CNN-U-Net | Proposed Framework |
|---|---|---|---|
| IoU (%) | 88.46 | 91.27 | **93.84** |
| Dice Score (%) | 91.72 | 94.18 | **96.12** |

| | | | |
|---|---|---|---|
| Pixel Accuracy (%) | 94.28 | 95.63 | **97.16** |
| Segmentation Precision (%) | 92.17 | 94.36 | **96.08** |
| Segmentation Recall (%) | 91.38 | 93.72 | **95.54** |

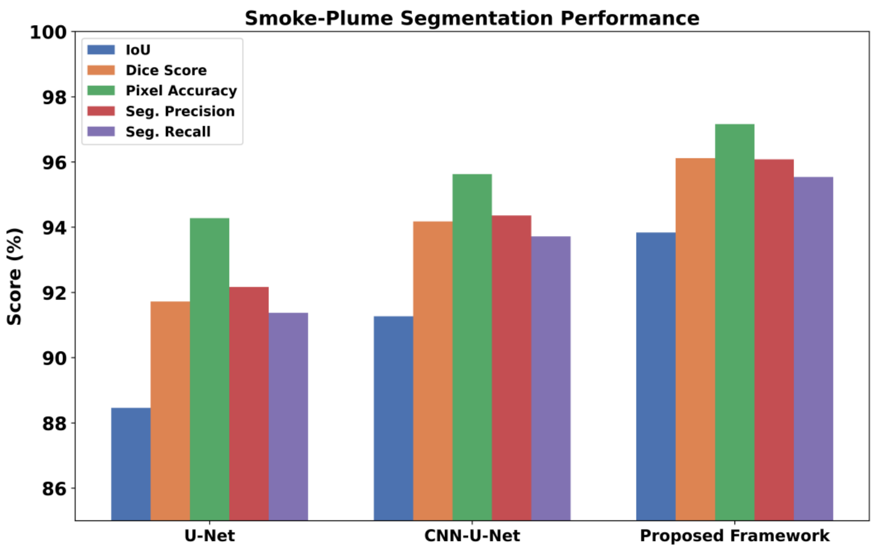


**Figure 5.** Smoke-Plume Segmentation Performance Comparison

Figure 5 shows grouped bar charts of IoU, Dice score, pixel accuracy, segmentation precision, and recall for U-Net, CNN-U-Net and proposed, where we can see that as we add more and more architectural components to the whole pipeline, the scores constantly improve for all five metrics.

**D. Air Pollution and Exposure Analysis**

The study provides a summary of accuracy of estimation of pollutants, including PM2.5, PM10, AOD and Air Quality Index (AQI). The RMSE and $R^2$ of the temporal module implemented using LSTM is 0.052 and 0.953, respectively, indicating that it has the lowest RE for AOD retrieval, as it has the most similar spectral relationship to satellite reflectance. The prediction of PM2.5 and AQI also have $R^2$ values greater than 0.93, showing good consistency with the ground-station observations despite the additional challenge of the conversion of aerosol levels to surface concentrations. The error of PM10 is slightly higher, in line with its higher sensitivity to dust and other non-fire particulate influences that it is not directly sensitive to by the fire sensitive feature extraction pipeline.

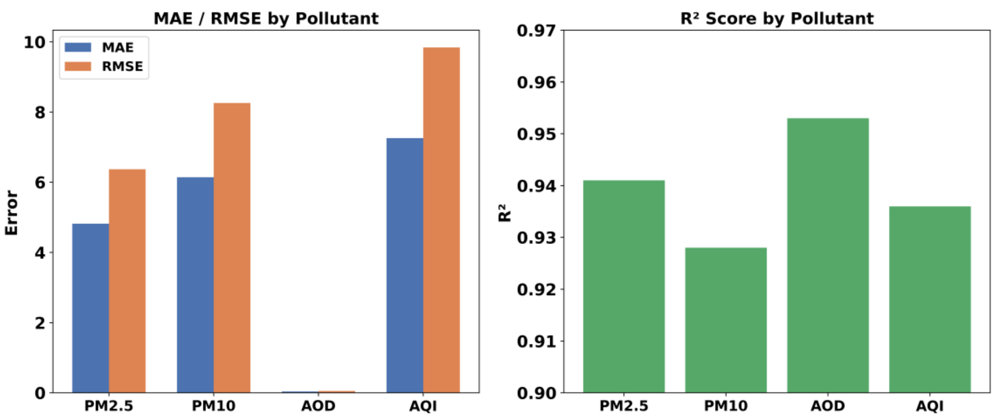


**Figure 6.** Air-Pollution Estimation Performance (MAE, RMSE, $R^2$)

Natural Resources for
Human Health
eISSN: 2583-1194

Figure 6 displays the bar charts of MAE/RMSE values along with the $R^2$ values for PM2.5, PM10, AOD and AQI, respectively, demonstrating that the estimation error is related to the variability of the pollutants, and the $R^2$ values are consistently well above 0.92, indicating reliable pollutant-concentration regression for all four measured atmospheric variables.

### E. Comparative Performance Analysis

In addition to the quantitative numbers, the intermediate representations, as shown qualitatively, further support the smoke sensitivity of the framework. The spatial region the network is paying attention to when detecting smoke- and fire-related features is shown in the raw spectral band panel (Figure 8) and in a heatmap of class-activation features (Figure 9), respectively.

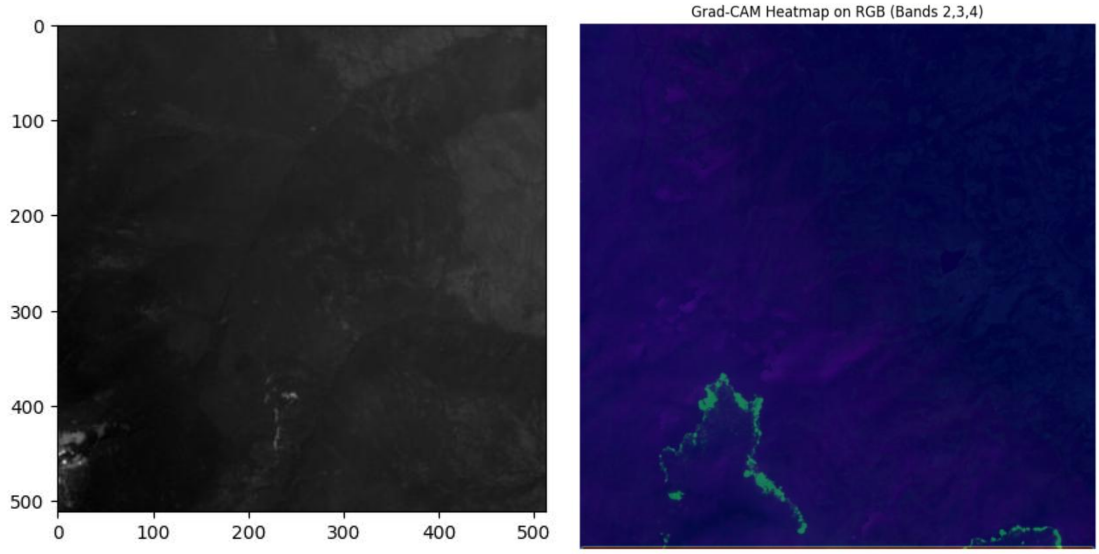


(a) (b)

**Figure 7.** (a) Single-Band Grayscale Reflectance Panel of the Input Scene (b) Grad-CAM Heatmap Overlaid on RGB Composite (Bands 2, 3, 4)

The single-band grayscale reflectance panel (shown in Figure 7, a), extracted from the input scene, has brighter areas in the lower-left as a result of surface reflectance levels associated with active burning or bare soil, and has a diagonal gradient across the frame, representing natural terrain reflectance and/or illumination variation across the tile. To see how the model is paying attention to the image, Figure 7 (b) shows the Grad-CAM activation heatmap overlaid on the RGB composite image, highlighting the green-shaded regions of the image which correspond to the image areas that most influenced the model's smoke-detection decision. Note that most of the green-shaded areas are clustered into a relatively small number of areas that form a spatially coherent, plume-shaped structure, and not spread throughout the image like random noise.

## VI. CONCLUSION AND FUTURE WORK

In this study, an integrated deep-learning framework for the mapping of forest-fire smoke, air pollution, and forest-fire human-health impacts is presented, based on the multispectral imagery provided by Sentinel-2 satellite. The proposed framework not only detected the pollution with a high accuracy of 96.75%, but also segmented the objects with a high IoU of 93.84% and successfully estimated the pollutants with high $R^2$ (above 0.92) for all pollutants measured; meanwhile, the framework could correctly classify the level of health risk with a 95.90% overall F1-score. The findings here validate the benefits of combining spatial, temporal and exposure information into a single pipeline as compared to single-task baselines, and represent a scalable approach to determining pollution hotspots and vulnerable populations during active fires. The framework is able to convert raw satellite reflectance straight to maps describing environmental risks to health, making it a usable decision-support tool for environmental agencies and public-health experts. The extension of the approach to include higher-frequency geostationary satellite observations for near real-time monitoring, to include meteorological wind-field data to enhance smoke-dispersion forecasting, and to validate health-risk predictions with clinical records of hospitalization over multiple fire seasons and geographic regions in the future. Further research will also be conducted on transformer architecture for temporal architectures, and uncertainty quantification for further enhancing robustness and reliability for operating use in early-warning systems.

**REFERENCES**

[1] Ghali, R., & Akhloufi, M. A. (2023). Deep Learning Approaches for Wildland Fires Using Satellite Remote Sensing Data: Detection, Mapping, and Prediction. Fire, 6(5), 192. https://doi.org/10.3390/fire6050192

[2] Elhanashi, A., Essahraui, S., Dini, P., & Saponara, S. (2025). Early Fire and Smoke Detection Using Deep Learning: A Comprehensive Review of Models, Datasets, and Challenges. Applied Sciences, 15(18), 10255. https://doi.org/10.3390/app151810255

[3] Yue, T., Huang, H., Wang, Q., Song, B., & Chen, Y. (2025). A Multimodal Deep Learning Framework for Accurate Wildfire Segmentation Using RGB and Thermal Imagery. Applied Sciences, 15(18), 10268. https://doi.org/10.3390/app151810268

[4] Bahadori, N., Razavi-Termeh, S. V., Sadeghi-Niaraki, A., Al-Kindi, K. M., Abuhmed, T., Nazeri, B., & Choi, S.-M. (2023). Wildfire Susceptibility Mapping Using Deep Learning Algorithms in Two Satellite Imagery Dataset. Forests, 14(7), 1325. https://doi.org/10.3390/f14071325

[5] Riaz Sheriff, Mohammad Suhail Meer, Rana Waqar Aslam, Yahia Said, Machine Learning-Based Forest Fire Susceptibility Mapping Using Random Forest and CART Models, Rangeland Ecology & Management, Volume 102, 2025, Pages 96-109, ISSN 1550-7424, https://doi.org/10.1016/j.rama.2025.06.004.

[6] Muthukumar, P., Nagrecha, K., Comer, D., Calvert, C. F., Amini, N., Holm, J., & Pourhomayoun, M. (2022). PM2.5 Air Pollution Prediction through Deep Learning Using Multisource Meteorological, Wildfire, and Heat Data. Atmosphere, 13(5), 822. https://doi.org/10.3390/atmos13050822

[7] Yu, S., & Singh, M. (2025). Deep Learning-Based Remote Sensing Image Analysis for Wildfire Risk Evaluation and Monitoring. Fire, 8(1), 19. https://doi.org/10.3390/fire8010019

[8] Shang, D., Zhang, F., Yuan, D., Hong, L., Zheng, H., & Yang, F. (2024). Deep Learning-Based Forest Fire Risk Research on Monitoring and Early Warning Algorithms. Fire, 7(4), 151. https://doi.org/10.3390/fire7040151

[9] Kim SY, Muminov A. Forest Fire Smoke Detection Based on Deep Learning Approaches and Unmanned Aerial Vehicle Images. Sensors (Basel). 2023 Jun 19;23(12):5702. doi: 10.3390/s23125702. PMID: 37420867; PMCID: PMC10304711.

[10] Durlević, U., Ilić, V., & Valjarević, A. (2025). Wildfire Susceptibility Mapping Using Deep Learning and Machine Learning Models Based on Multi-Sensor Satellite Data Fusion: A Case Study of Serbia. Fire, 8(10), 407. https://doi.org/10.3390/fire8100407

[11] Vasconcelos, R. N., Franca Rocha, W. J. S., Costa, D. P., Duverger, S. G., Santana, M. M. M. d., Cambui, E. C. B., Ferreira-Ferreira, J., Oliveira, M., Barbosa, L. d. S., & Cordeiro, C. L. (2024). Fire Detection with Deep Learning: A Comprehensive Review. Land, 13(10), 1696. https://doi.org/10.3390/land13101696

[12] Aajila, J., & Kannan, E. P. (2026). LG Fusion++: Adaptive Nonlinear Frequency-Aware and Task-Driven Multimodal Image Fusion. International Journal on Advanced Computer Engineering and Communication Technology, 15(2), 136–143. Retrieved from https://journals.mriindia.com/index.php/ijacect/article/view/3630

[13] Sathishkumar, V.E., Cho, J., Subramanian, M. et al. Forest fire and smoke detection using deep learning-based learning without forgetting. fire ecol 19, 9 (2023). https://doi.org/10.1186/s42408-022-00165-0

[14] Akhyar, A., Lee, J., Shahar, N. et al. Automated forest fire detection in ecological monitoring using enhanced deep learning networks. Sci Rep 16, 2039 (2026). https://doi.org/10.1038/s41598-025-31707-6

[15] Patil, A., & Patil, P. (2025). Air Quality Index Prediction using Machine Learning. International Journal on Advanced Computer Theory and Engineering, 14(1), 43–47. https://doi.org/10.65521/ijacte.v14i1.211

[16] Das, K., Flesca, S. & Calidonna, C.R. Quantifying wildfire impacts on atmospheric pollutants using fire exposure metrics and machine–deep learning approaches. Sci Rep 16, 21234 (2026). https://doi.org/10.1038/s41598-026-51766-7